RNA (1997), 3:405–419. Cambridge University Press. Printed in the USA.

A highly stable duplex structure sequesters the 5′ splice site region of hnRNP A1 alternative exon 7B

MARCO BLANCHETTE and BENOIT CHABOT

Département de Microbiologie et Infectiologie, Faculté de Médecine, Université de Sherbrooke, Sherbrooke, Québec, Canada J1H 5N4

ABSTRACT

Exon 7B in the hnRNP A1 pre-mRNA is alternatively spliced to yield A1 and $A1^B$, two proteins that differ in their ability to modulate 5′ splice site selection. Sequencing the murine intron downstream of exon 7B revealed the existence of several regions of similarity to the corresponding human intron. In vitro splicing assays indicate that an 84-nt region (CE6IO) decreases splicing to the proximal 5′ splice site in a pre-mRNA carrying the 5′ splice sites of exon 7 and 7B. In vivo, the CE6IO element promotes exon 7B skipping in pre-mRNAs expressed from a mini-gene containing the hnRNP A1 alternative splicing unit. Using oligonucleotide-targeted RNase H cleavage assays, we provide support for the existence of highly stable base pairing interactions between CE6IO and the 5′ splice site region of exon 7B. Duplex formation occurs in naked pre-mRNA, resists incubation in splicing extracts, and is associated with a reduction in the assembly of U1 snRNP-dependent complexes to the 5′ splice site of exon 7B. Our results demonstrate that pre-mRNA secondary structure plays an important role in promoting exon 7B skipping in the A1 pre-mRNA.

Keywords: RNA structure; splice site selection; splicing; U1 snRNP

INTRODUCTION

The selection of splice sites in messenger RNA precursors (pre-mRNAs) is accomplished through the participation of several *cis* and *trans*-acting elements. Initially, the 5′ and 3′ splice sites are recognized by U1 snRNP and $U2AF^{65}$, respectively. Additional elements and factors also influence the interactions of U1 snRNP and $U2AF^{65}$ with splicing signals (reviewed in Black, 1995; Reed, 1996). Factors that improve splice site recognition include members of the SR family of proteins (reviewed in Fu, 1995; Chabot, 1996; Manley & Tacke, 1996). The SR protein SF2/ASF stimulates U1 snRNP binding to 5′ splice sites (Eperon et al., 1993), a process mediated through an interaction with the U1 snRNP 70K protein (Wu & Maniatis, 1993; Kohtz et al., 1994). Constitutive and regulated splicing enhancers bound by SR proteins can also improve 3′ splice site recognition by $U2AF^{65}$ (Lavigueur et al., 1993; Wang et al., 1995; Zuo & Maniatis, 1996). In this case, the assembly of an enhancer complex containing $U2AF^{35}$ recruits $U2AF^{65}$ through SR/$U2AF^{35}$/$U2AF^{65}$ protein–protein interactions (Wu & Maniatis, 1993; Zuo & Maniatis, 1996). SR proteins are also required when a U1-bound 5′ splice site stimulates upstream 3′ splice site utilization through exon-bridging interactions (Robberson et al., 1990; Wang et al., 1995). The best examples documenting the negative regulation of U1 snRNP and $U2AF^{65}$ binding have been described in *Drosophila*. In the case of the P-element pre-mRNA, sequences upstream of the germ-line-specific 5′ splice site promote the assembly of a complex containing U1 snRNP, hrp48, and the soma-specific protein PSI that prevents U1 snRNP binding at the authentic site (Siebel et al., 1994, 1995). In the case of the male-specific 3′ splice site of *transformer*, $U2AF^{65}$ binding is down-regulated by *sex lethal* (Valcárcel et al., 1993). A similar task may be accomplished by the mammalian PTB protein during α-tropomyosin pre-mRNA splicing (Lin & Patton, 1995). Finally, the effect of SR proteins on mammalian 5′ splice site selection is counteracted with different efficiencies by the heterogeneous ribonucleoparticle (hnRNP) A1, $A1^B$, A2, and B1 proteins (Mayeda & Krainer, 1992; Cáceres et al., 1994; Mayeda et al., 1994; Yang et al., 1994). How hnRNP proteins impose distal 5′ splice site selection remains to be determined.

Reprint requests to: Benoit Chabot, Département de Microbiologie et Infectiologie, Faculté de Médecine, Université de Sherbrooke, 3001 12e Avenue Nord, Sherbrooke, Québec, Canada J1H 5N4; e-mail: b.chabot@courrier.usherb.ca.

In addition to the interactions of *trans*-acting factors, specific RNA–RNA interactions occurring within the pre-mRNA also play a role in splicing by influencing the presentation of splicing signals to components of the splicing machinery. Artificial or natural occurrences of internal duplexes can influence splice site selection and splicing efficiency. In yeast, plants, and mammals, the utilization of splice sites can be prevented by placing the sites within a loop (Solnick, 1985) or by sequestering the sites within a stem (Eperon et al., 1986; Solnick & Lee, 1987; Fu et al., 1988; Clouet d'Orval et al., 1991a, 1991b; Deshler & Rossi, 1991; Goguel et al., 1993; Vilardell & Warner, 1994; Liu et al., 1995). Secondary structures can also have a positive influence on splicing by reducing the spacing between splicing signals (Chebli et al., 1989; Goguel & Rosbash, 1993; Libri et al., 1995; Charpentier & Rosbash, 1996), or by facilitating the presentation of splice sites (Newman, 1987; Domenjoud et al., 1991; Kister et al., 1993).

The hnRNP A1 pre-mRNA contains an alternative exon (7B) that is either included to produce $A1^B$ or excluded to yield A1 (Buvoli et al., 1990). With the aim of understanding how the alternative splicing of A1 pre-mRNA is modulated, we have initiated an investigation to identify pre-mRNA sequences, other than splicing signals, that are involved in splice site utilization. Toward that goal, we have recently uncovered a conserved intron element (CE1) located upstream of the alternative exon 7B that promotes distal 5′ splice site selection but does not affect U1 snRNP binding (Chabot et al., 1997). Here, we report the existence of another conserved intron element (CE6IO) located downstream of exon 7B. CE6IO promotes distal 5′ splice site selection by forming a secondary structure with the 5′ splice site region of exon 7B, thereby reducing the assembly of U1-dependent complexes. Taken together, our results indicate that the alternative splicing of hnRNP A1 exon 7B is modulated by distinct intron elements acting through different mechanisms.

RESULTS

Evolutionary conserved elements in intron 7B

As part of a study aimed at understanding how splicing of the alternative exon 7B is modulated, we sequenced the intron separating exons 7B and 8 using a genomic copy of the mouse A1 gene isolated previously (Ben-David et al., 1992). Comparing the sequence of intron 7B with the corresponding human intron revealed that, in addition to sequence similarity at the 5′ splice site region, intron 7B contained several stretches of conserved nucleotides scattered throughout the intron (Fig. 1). Although the length of conserved elements (CE) varies considerably, a 41-nt region designated CE6 displays the most extensive level of conservation between the murine and human intron (95%). Although an overall conservation of 60% in intron 7B is not as dramatic as the conservation observed for intron 7 (75%), it remains greatly superior to the conservation of intron 6 (25%), which separates constitutive exons 6 and 7 (Chabot et al., 1997). The extensive sequence similarity between the human and murine intron 7B suggests that the conserved regions may play a role in modulating the alternative splicing of exon 7B. Indeed, this prediction was recently fulfilled for the CE1 element located in the hnRNP A1 intron 7 (Chabot et al., 1997).

CE6IO element promotes distal 5′ splice site selection and exon 7B skipping

To test the effect of some of the conserved sequences of intron 7B on 5′ splice site selection, we performed splicing reactions in HeLa nuclear extracts. As a model pre-mRNA substrate, we used a hybrid RNA containing the 5′ splice site of exons 7 and 7B in competition for the 3′ splice site of the adenovirus L2 exon (S1 RNA; Fig. 2A). S1 RNA was spliced preferentially to the proximal 5′ splice site of exon 7B (Fig. 2B, lane 1). When a region corresponding to the 200-bp *Stu* I fragment (STE element, see Fig. 1) was inserted at its natural position downstream of exon 7B, splice site selection shifted to the upstream 5′ splice site of exon 7 (S678 RNA; Fig. 2B, lane 3). In contrast, when the STE element was inserted in the reverse orientation, each 5′ splice site was used with approximately equivalent efficiency (S678i RNA; Fig. 2B, lane 2).

The STE element contains several stretches of conserved nucleotides. To identify sequences within STE responsible for activating the distal 5′ splice site, we substituted the STE element with smaller regions corresponding to some of the most conserved stretches in STE. The first half of the STE element (CE6IO, see Fig. 1) possessed all the information required to favor distal 5′ splice site selection (SCE6IO RNA; Fig. 2B, lane 5). In contrast, a control pre-mRNA containing the complementary sequence of CE6IO was spliced considerably more efficiently to the proximal 5′ splice site (SCE6IOi RNA; Fig. 2B, lane 4). Insertion of CE6, a subfragment of CE6IO, only had a minor effect on splice site selection (SCE6 RNA, Fig. 2B, lane 6), as judged by comparison with SCE6i RNA, which carries the complementary sequence of CE6 (lane 7). However, the modest contribution of CE6 was found to be significant because a pre-mRNA lacking the last 7 nt of CE6 (SCE6Δ RNA) was spliced more efficiently to the proximal 5′ splice site (Fig. 2B, lane 8), a profile comparable to SCE6Δi RNA, which contains the same element in the reverse orientation (lane 9). In contrast, the splicing profile of pre-mRNAs containing either CE7 or CE8 was identical to the splicing profile of pre-mRNAs containing the complementary sequence of CE7 or CE8 (Fig. 2B, lanes 10–13). Thus, our analysis

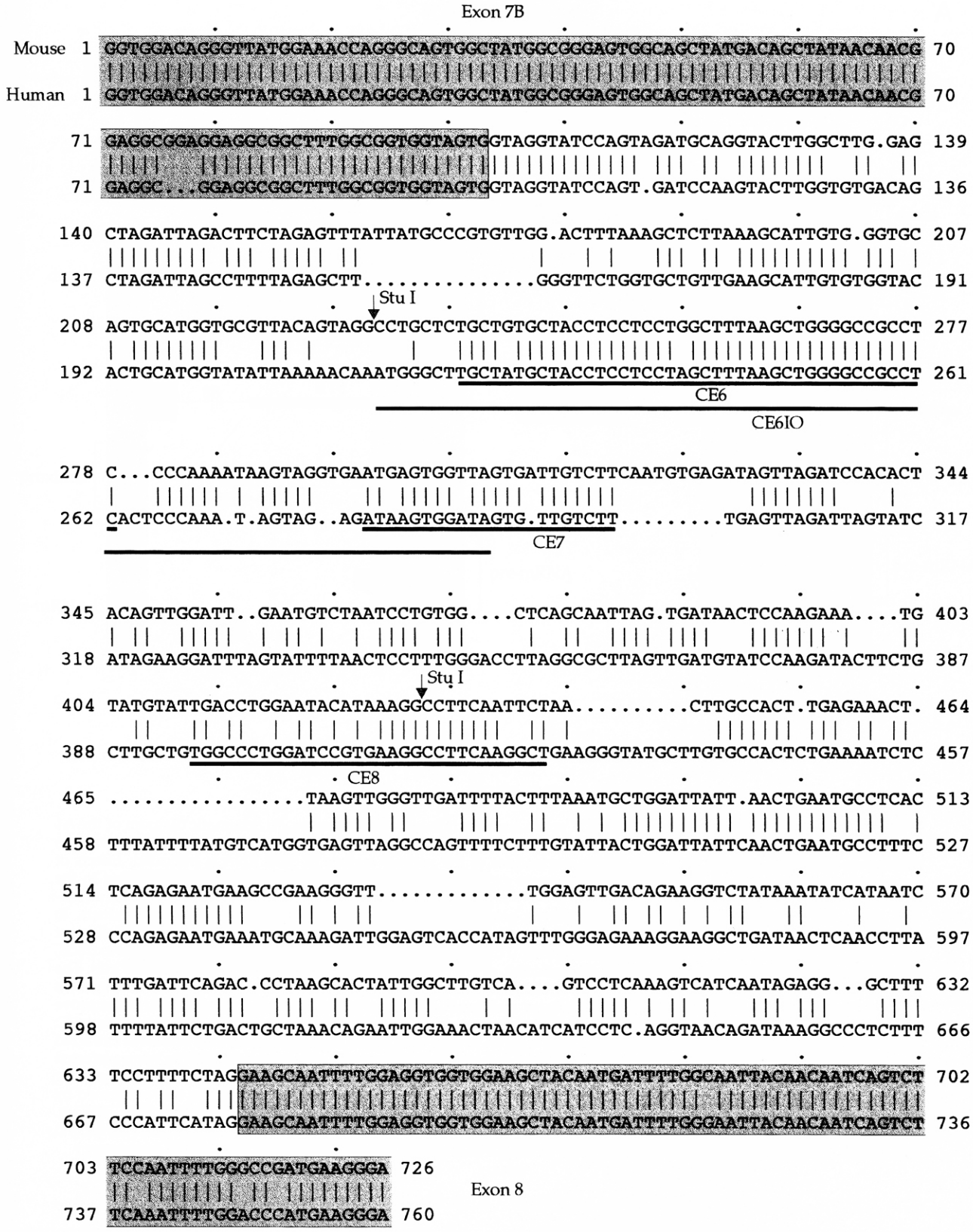

FIGURE 1. Sequence of the mouse and human hnRNP A1 alternative splicing unit. A portion of the mouse hnRNP A1 gene (top) extending from alternative exon 7B to exon 8 was sequenced and compared to the corresponding region of the human A1 gene (bottom; [Biamonti et al., 1989]). Exon sequences are represented by shaded boxes. Alignment was made using the GAP program of the Genetics Computer Group (University of Wisconsin Biotechnology Center) and was further optimized by eye. The CE6, CE6IO, CE7, and CE8 conserved intron elements are underlined. Within the mouse intron 7B, the 200 bp *Stu* I fragment corresponds to the STE element.

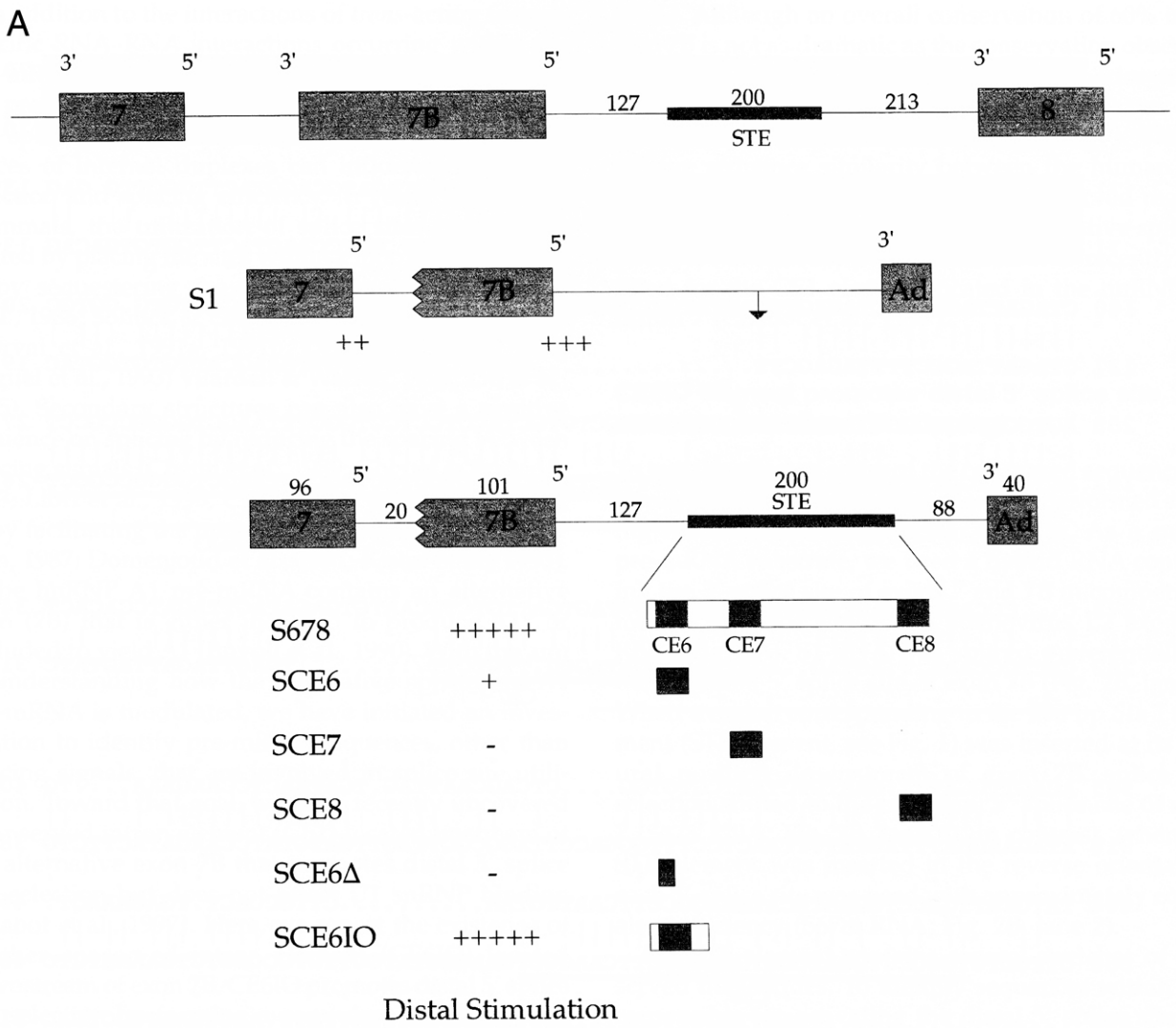

FIGURE 2. An intron element promotes distal 5′ splice site selection and exon skipping. **A:** Schematic diagram of the A1 alternative splicing unit with the position of the STE element (top). Also shown are the structure of S1, S678, and various derivatives tested for splicing in B. The size in nucleotides of the various regions of S678 RNA is indicated. Effects of conserved elements on distal 5′ splice site selection are expressed relative to the effect of each element inserted in the reverse orientation: − represents no difference; +++++ represents the maximal shift toward distal 5′ splice site utilization. These values were obtained by scanning splicing gels to obtain the ratio of distal to proximal lariat products. **B:** ^{32}P-labeled RNA substrates were synthesized from plasmids lacking STE (S1 RNA), containing the complete STE element (S678 RNA) or portions of STE in the sense and antisense (i derivatives) orientation. Following incubation in HeLa extracts, splicing products were loaded onto 8% (left), 6% (middle), or 7% (right) acrylamide/8 M urea/30% formamide gels. The relative frequencies of distal and proximal splice site utilization were estimated by comparing the intensity of the bands derived from proximal and distal lariat intermediates and products that migrate above the pre-mRNAs. To improve resolution of lariat species, gels were run extensively accounting for the absence of the mRNA and the 5′ exon. **C:** Forty-eight hours following transfection of HeLa and WI38VA13 cells with pmA1 and derivatives, total RNA was extracted and a RT-PCR assay was performed to analyze splicing products derived from the mini-genes. RNA from nontransfected cells was used as a control (lanes 3 and 7). PCR assays were performed on pCMV derivatives carrying the corresponding portion of the A1 (lane 1) or A1^{B} (lane 2) cDNA. The identity of the A1^{B} band in transfected samples was confirmed by restriction enzyme digestion. **D:** Structure of the A1 mini-gene and derivatives. pmA1ΔSTE lacks the STE element. pmA1STEi contains the STE element in the reverse orientation. pmA1Δ1 contains the CE6IO element but lacks the second half of STE. The position of oligonucleotides used in the RT-PCR assays is indicated. (*Figure continues on facing page.*)

identified a region in intron 7B that improves selection of the 5′ splice site of exon 7, raising the possibility that the 84-nt CE6IO element plays a role in promoting exon 7B skipping in the A1 pre-mRNA.

To address the contribution of STE and CE6IO in the alternative splicing of hnRNP A1 exon 7B, we tested the effect of these elements in their natural context in vivo. A mini-gene carrying a genomic portion of the mouse A1 gene (pmA1, Fig. 2D) was expressed transiently in HeLa and WI38VA13 cells. RT-PCR analysis indicated that A1 transcripts derived from pmA1 were spliced preferentially to yield RNAs lacking exon 7B

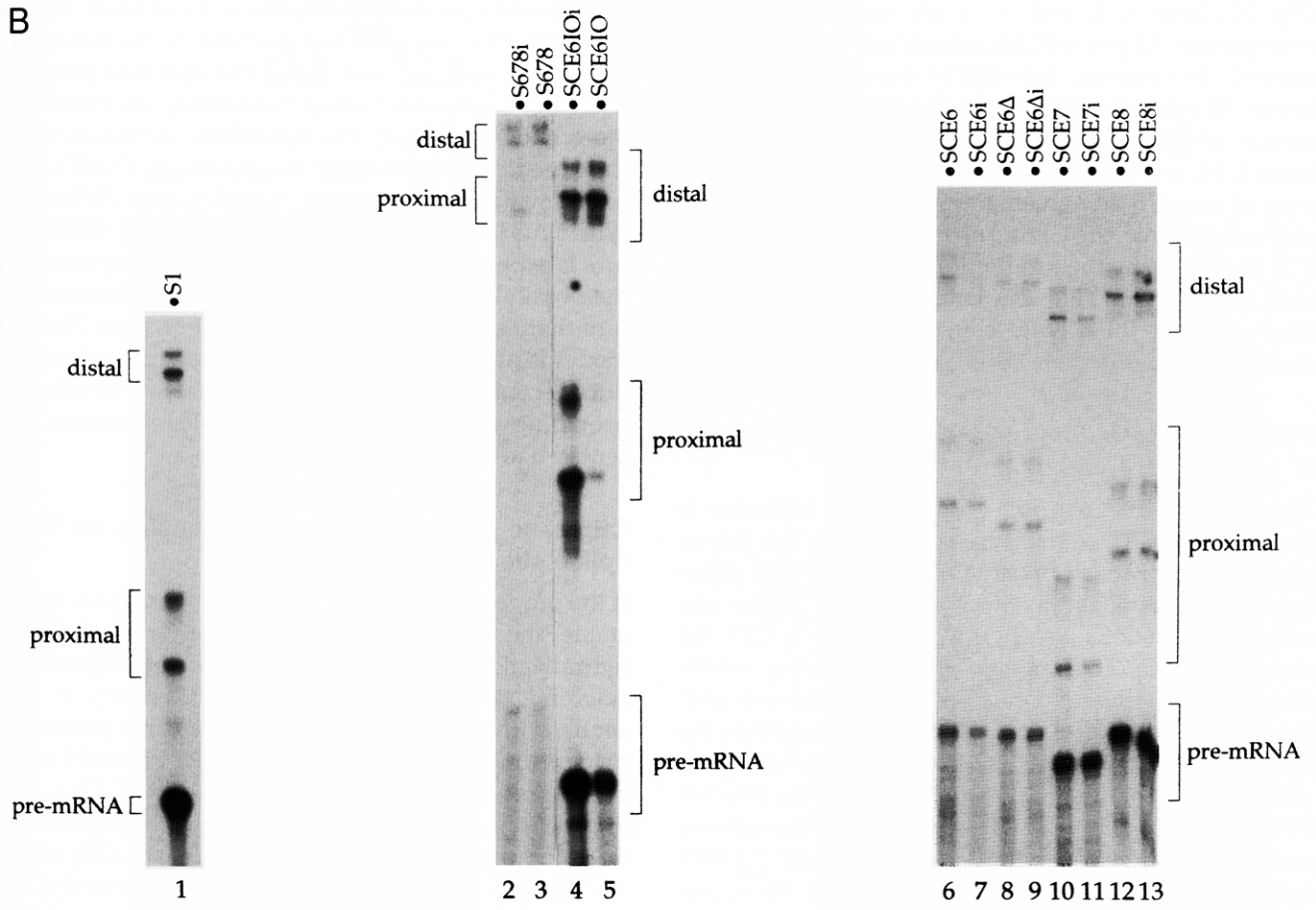

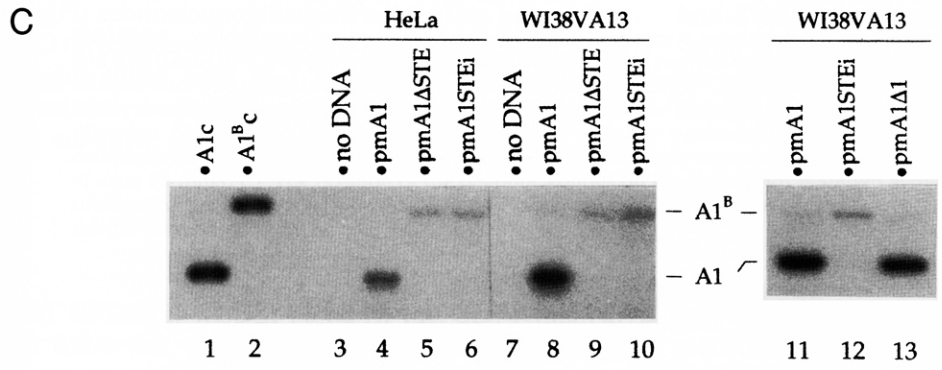

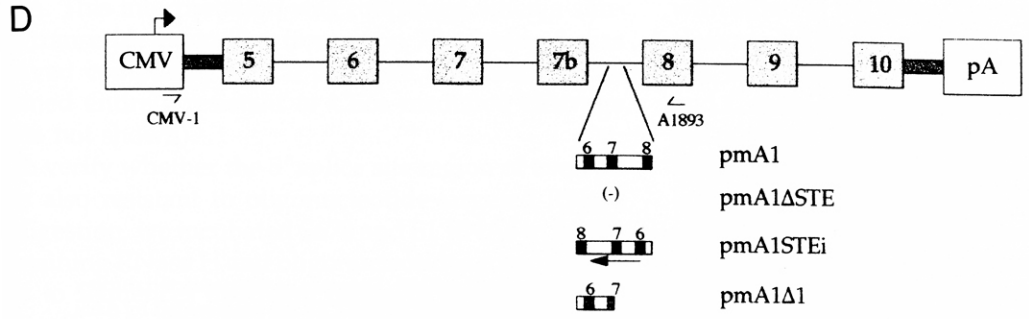

FIGURE 2. *Continued.*

(Fig. 2C, lanes 4, 8, and 11), a fate comparable to the endogenous A1 pre-mRNA in both cell lines (data not shown). In contrast, deletion of the STE element in intron 7B (pmA1ΔSTE; Fig. 2C, lanes 5 and 9), or insertion of STE in the reverse orientation (pmA1STEi; lanes 6, 10, and 12), almost completely eliminated skipping of exon 7B. In agreement with the in vitro results presented above, the CE6IO element was as efficient as STE at promoting the production of transcripts lacking exon 7B (pmA1Δ1; Fig. 2C, lane 13). This study demonstrates that the CE6IO element in intron 7B promotes skipping of exon 7B in vivo.

Possible base pairing between CE6IO and the 5′ splice site region of exon 7B

The effect of CE6IO on splice site selection is similar to the effect of CE1, a conserved element in the intron upstream of exon 7B (Chabot et al., 1997). CE1 interacts with hnRNP A1 to promote distal 5′ splice site selection and exon 7B skipping. In contrast to CE1, the sequence of CE6IO lacks hnRNP A1 binding motifs ($UAGGG^{U}/_{A}$) (Burd & Dreyfuss, 1994). Moreover, adding a large excess of STE RNA did not antagonize the effect of a *cis*-acting STE on 5′ splice site selection in vitro (data not shown). The possibility that the effect of STE on splice site selection may be conformational was suggested by the following observations: (1) S678 and SCE6IO RNAs, but not S678i or STE RNA, migrated abnormally in acrylamide/8 M urea gels, despite prior boiling of the RNAs in 100% formamide (data not shown); (2) proper migration of S678 and SCE6IO RNAs was restored by including 30% formamide in the urea gel (Fig. 2B). These observations are consistent with the existence of an unusually stable secondary structure in S678 RNA.

To identify pre-mRNA sequences most likely to base pair with STE, we analyzed portions of the mouse A1 alternative splicing unit using the MFOLD program (Genetics Computer Group, University of Wisconsin Biotechnology Center). The most stable secondary structure predicted implicated sequences of CE6IO base paired with the 5′ splice site region of exon 7B (Fig. 3). With a ΔG° of approximately −45 kcal/mol, this structure is expected to be highly stable. This analysis raises the possibility that CE6IO forms a highly stable structure that sequesters the 5′ splice site of exon 7B. This model is attractive because duplex formation may reduce U1 snRNP binding to the 5′ splice site of exon 7B, providing an explanation for the splicing results presented above.

CE6 base pairs with sequences flanking the 5′ splice site of exon 7B

If the proposed secondary structure exists and is highly stable, the CE6 sequence should not be accessible to hybridization with a complementary deoxyoligonucleotide and, consequently, should be refractory to subsequent RNase H digestion. We tested this possibility by performing oligonucleotide-targeted RNase H cleavage assays in buffer alone (Fig. 4A). S678 RNA was incubated in the presence of RNase H and oligonucleotides complementary to either CE6, CE7, or CE8 (oligonucleotides CE6a, CE7a, and CE8a, respectively). As controls, parallel incubations were performed with STE RNA. Whereas STE RNA was cleaved efficiently in the presence of each of the three oligonucleotides (Fig. 4A, lanes 10–12), S678 RNA was digested readily with CE7a, but not with CE6a (lanes 1–6). This result suggests that the CE6 region is not available for hybridization with oligonucleotide CE6a, consistent with the pro-

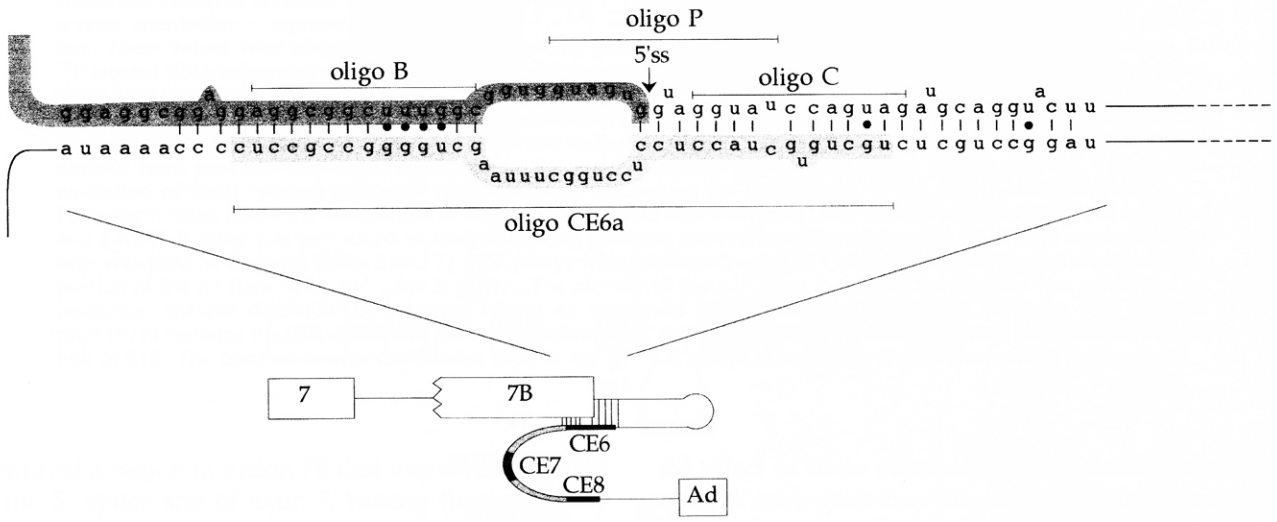

FIGURE 3. Predicted secondary structure of a portion of the STE-containing pre-mRNA. Diagram of the predicted duplex formed between CE6IO and the 5′ splice site region of exon 7B. The sequences of exon 7B and CE6 are represented by dark and light shaded boxes, respectively. The position of various oligonucleotides used in this study is indicated above and below the sequence. The sequence of each oligonucleotide is complementary to the region indicated by brackets.

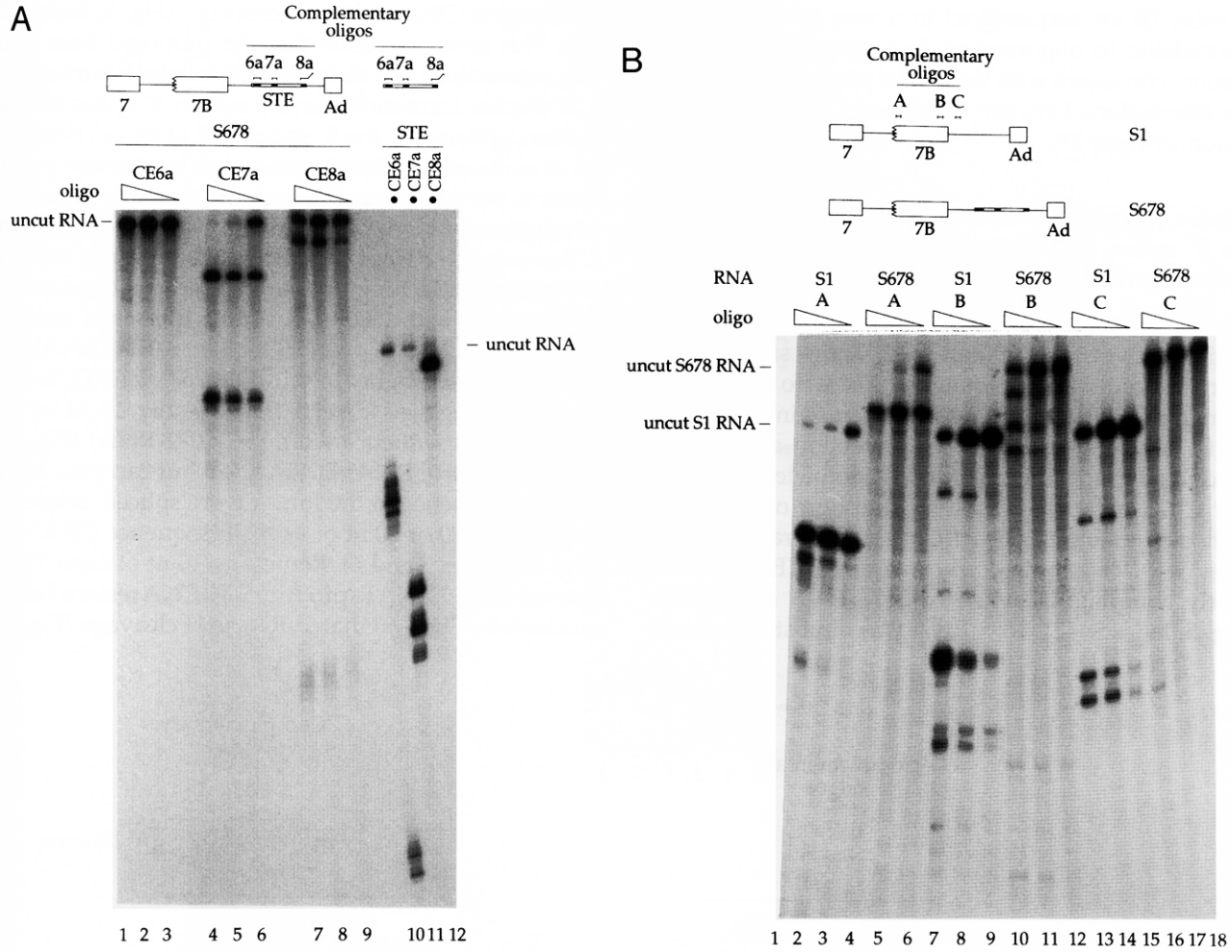

FIGURE 4. Validation of the structural model. **A:** CE6 sequence is resistant to RNase H digestion. Labeled S678 (lanes 1–9) and STE (lanes 10–12) RNAs were incubated in the absence of nuclear extracts, but in the presence of RNase H and various concentrations of oligonucleotides complementary to CE6, CE7, or CE8. The structure of the RNA tested and the position of the complementary oligonucleotides are indicated. **B:** The 5′ splice site region of exon 7B is resistant to RNase H digestion. S1 and S678 RNAs were incubated as in A, in the presence of increasing concentrations of oligonucleotides complementary to exon 7B sequences (oligos A and B) and intron sequences immediately downstream of the 5′ splice site of exon 7B (oligo C). The position of the oligonucleotides on the pre-mRNA is shown above (see Fig. 3B). The position of undigested pre-mRNAs is shown in A and B. Note that the smallest cleavage product generated with oligo A ran out of the gel (lanes 1–6).

posed structural model. Notably, the CE8 region in S678 RNA was cleaved only partially by RNase H (Fig. 4A, lanes 7–9). Because S678 RNA contains only a portion of the CE8 sequence, partial cleavage may be due to the imperfect hybridization of CE8a to S678 RNA. This interpretation was confirmed when a simple transcript extending from exon 7B to exon 8 was cleaved completely in the presence of CE8a, but remained entirely resistant to CE6a-mediated cleavage (data not shown).

To verify whether the 5′ splice site region of exon 7B was also resistant to oligonucleotide-targeted RNase H digestion, we incubated S678 and S1 RNAs in buffer containing RNase H and oligonucleotides complementary to sequences upstream (oligo B) or downstream (oligo C) of the 5′ splice site of exon 7B (Fig. 4B). Based on the model proposed in Figure 3, the exon and intron sequences targeted by these oligonucleotides are predicted to base pair with CE6 in S678, but not in S1 RNA. As a control, we used an oligonucleotide complementary to the upstream portion of exon 7B sequences in S678 and S1 RNAs (oligo A). Incubations with either of the three oligonucleotides led to efficient cleavage of S1 RNA (Fig. 4B, lanes 1–3, 7–9, and 13–15). In contrast and as predicted, oligonucleotides B and C were unable to direct cleavage of S678 RNA at the targeted positions (Fig. 4B, lanes 10–12 and 16–18, respectively). The bands obtained with oligo B (Fig. 4B, lanes 10–12) did not match the size of the predicted products and are likely produced from cleavages in exon regions with limited complementarity to oligo B. As expected, oligo A induced cleavage of S678 RNA as efficiently as in S1 RNA (Fig. 4B, lanes 4–6). Our results indicate that sequences flanking the 5′ splice site

of exon 7B are sequestered in a way to render them unavailable to oligonucleotide-targeted RNase H digestion, consistent with the model proposing base pairing interactions between CE6IO and the 5′ splice site region of exon 7B.

Duplex formation between CE6IO and the 5′ splice site region of exon 7B occurs in nuclear extracts

The results presented above suggest that duplex formation between CE6IO and the 5′ splice site region of exon 7B occurs readily in naked RNA. To address the formation and stability of this structure in nuclear extracts, time-course RNase H protection assays were conducted in splicing mixtures. Oligonucleotides CE6a and CE7a targeted RNase H digestion of STE RNA with similar efficiencies in nuclear extracts (Fig. 5, lanes 1–8). In contrast, whereas oligo CE7a induced nearly complete cleavage of S678 RNA at all times (Fig. 5, lanes 9–12), S678 RNA was almost completely resistant to CE6a-mediated cleavage (Fig. 5, lanes 12–16). This result suggests that the proposed base pairing interactions are also stable in nuclear extracts.

If duplex formation plays a role in 5′ splice site selection, splicing to the 5′ splice site of exon 7B should be stimulated by deleting the exon sequences postulated to participate in duplex formation. We tested this prediction by monitoring splicing and oligonucleotide CE6a-targeted RNase H cleavage of simple pre-mRNAs containing or lacking the exon 7B sequences proposed to base pair with CE6IO. A simple transcript containing STE and 20 nt of exon 7B sequence (ST-1 RNA) was not spliced detectably in vitro (Fig. 6A, lane 1). In contrast, splicing was detected when only 10 nt of upstream exon sequence were left (ST-2 RNA) (Fig. 6A, lane 2). Control RNAs lacking STE but carrying 150 nt of filler sequence in the intron were spliced efficiently with either 20 or 10 nt of exon 7B sequence (SF RNAs; Fig. 6A, lanes 3 and 4). Removing 10 nt of exon 7B sequence in ST-1 RNA to produce ST-2 RNA restored oligonucleotide CE6a-mediated RNase H cleavage (Fig. 6B,

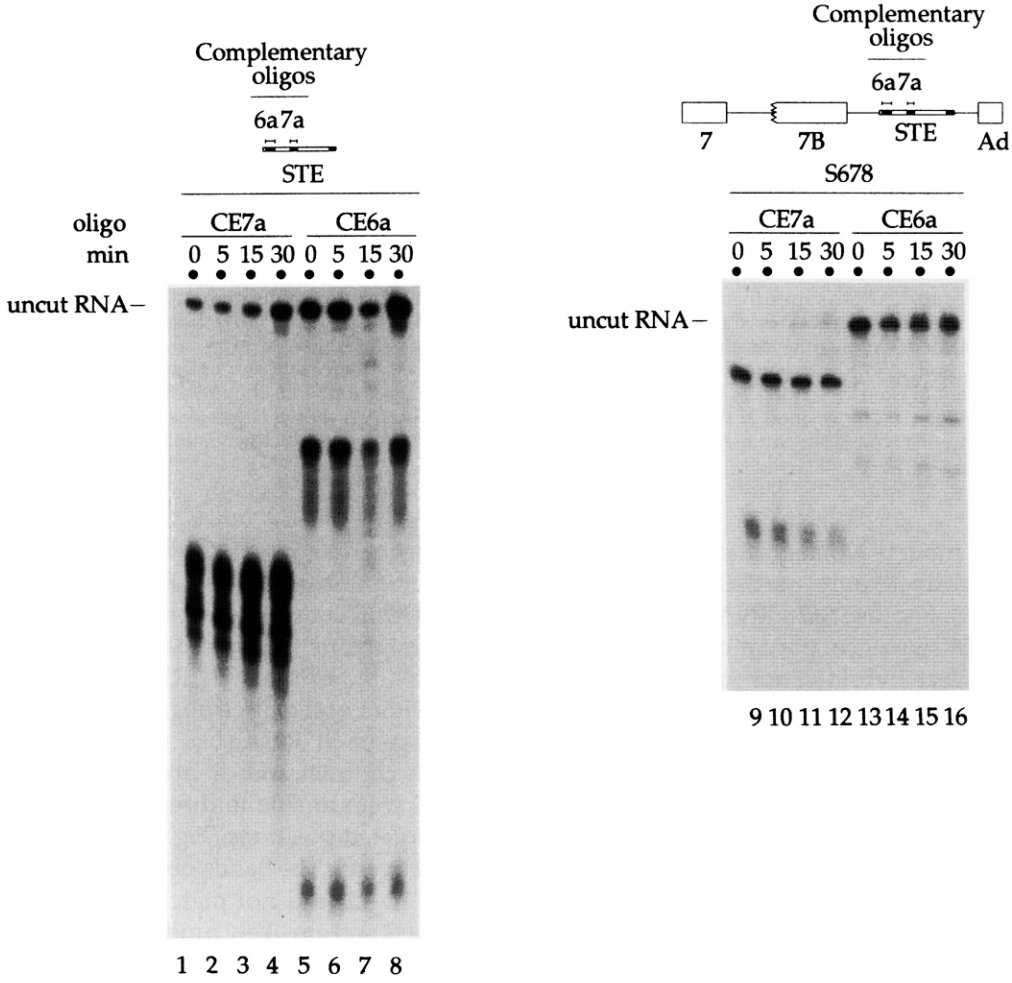

FIGURE 5. Duplex formation in nuclear extracts. STE and S678 RNAs were incubated at 30 °C in nuclear extracts for the indicated times (in min) and submitted to RNase H digestion in the presence of oligonucleotides CE6a or CE7a. The position of the uncut RNAs is indicated.

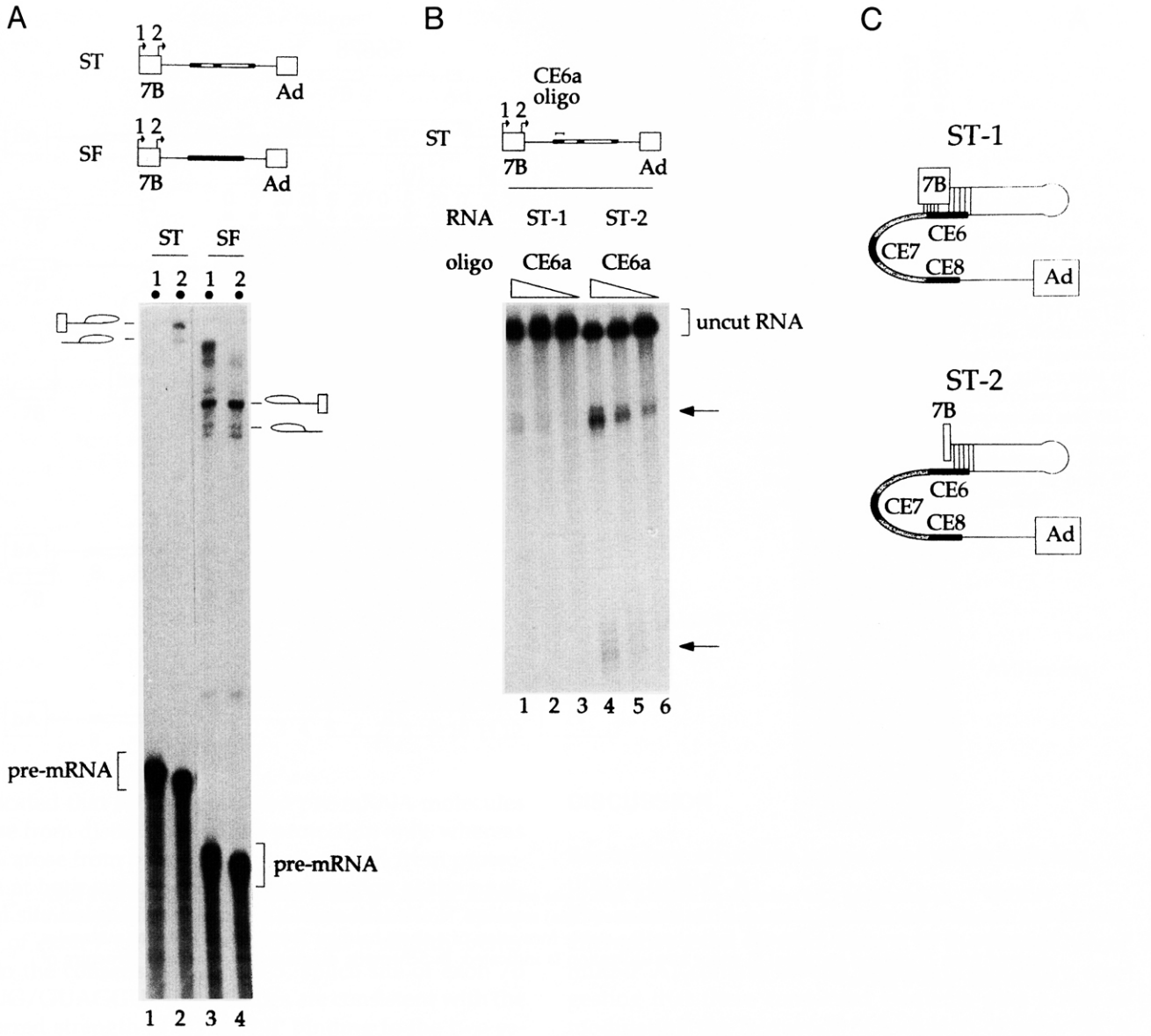

FIGURE 6. Exon sequences upstream of the 5′ splice site of exon 7B inhibit splicing and affect the availability of the CE6 sequence. **A:** Simple pre-mRNAs containing (ST-1, SF-1) or lacking (ST-2, SF-2) exon sequences postulated to base pair with CE6 were incubated in splicing mixtures for 2 h at 30 °C. ST RNAs contain the STE element, whereas the SF RNAs contain 150 nt of filler sequence. **B:** CE6a oligonucleotide-targeted RNase H digestion of ST RNAs, as performed in Figure 5. Arrows indicate the position of cleavage products. **C:** Schematic diagram of the duplex structures postulated to form in ST-1 and ST-2 RNAs.

lanes 1–6). Thus, our results suggest that base pairing between CE6IO and exon 7B sequences are important for splicing inhibition. In the absence of these interactions, the remaining complementarity between CE6IO and intron sequences downstream of the 5′ splice site of exon 7B does not appear sufficient to block splicing in vitro.

Restoration of proximal 5′ splice site selection in the presence of STE

Another prediction from the structural model is that sequestering CE6IO in an alternate duplex structure should activate splicing to exon 7B. This prediction was verified by including into S678 RNA a sequence complementary to CE6 (S6a678 RNA, Fig. 7B). The migration of S6a678 RNA was retarded considerably in a gel containing urea and formamide (Fig. 7A, lane 4), consistent with the presence of a highly stable duplex hairpin. The presence of the CE6a sequence was associated with more efficient splicing to the 5′ splice site of exon 7B. The CE6/CE6a duplex did not affect the migration of lariat molecules significantly, possibly because the contribution of the duplex was offset by the bulkier lariat structure. As a control, CE6 was inserted in the sense orientation, allowing duplex

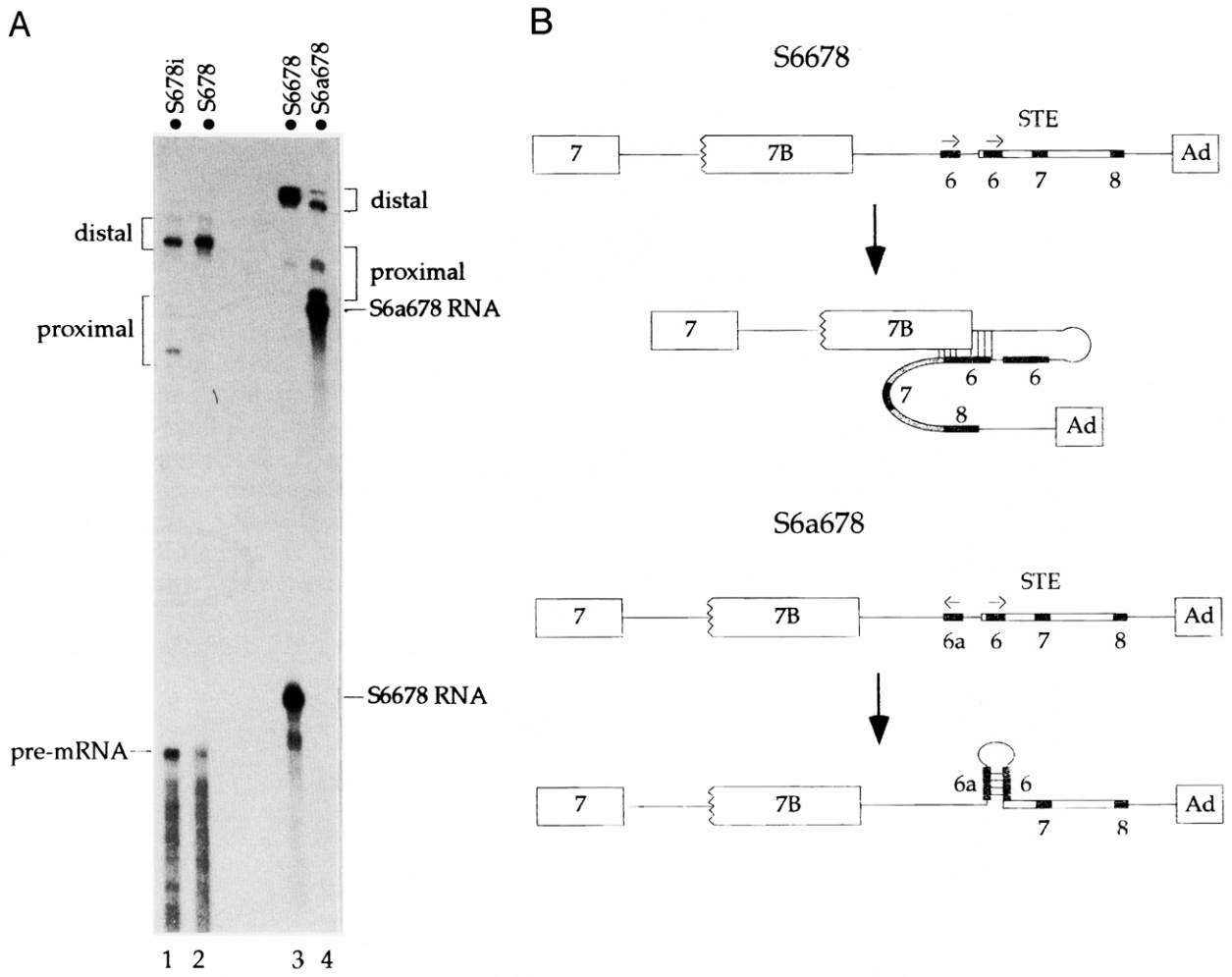

FIGURE 7. Sequestering CE6 activates proximal 5′ splice site selection. **A:** Splicing assays were performed with S678 RNA and derivatives containing the CE6 and CE6 antisense (CE6a) sequence. Note that insertion of CE6a promotes the aberrant migration of the pre-mRNA (lane 4), indicating the stable formation of a short hairpin. The position of lariat molecules derived from distal and proximal 5′ splice site utilization is indicated. **B:** Schematic diagram and predicted structure of S6678 and S6a678 RNAs.

formation to occur with either the newly added CE6 or the original CE6IO element (S6678 RNA, Fig. 7B). S6678 RNA was spliced almost exclusively to the distal 5′ splice site (Fig. 7A, lane 3). Thus, the effect of CE6IO in splice site selection can be neutralized by providing in *cis* a sequence that hybridizes to CE6, reducing the probability of base pairing with the 5′ splice site region of exon 7B.

Duplex formation reduces the assembly of U1-dependent complexes

Duplex formation between CE6IO and the 5′ splice site region of exon 7B may prevent efficient U1 snRNP binding, leading to an increase in the selection of the 5′ splice site of exon 7. To ascertain whether duplex formation affects the assembly of complexes on the 5′ splice site of exon 7B, we performed an RNase H cleavage assay in HeLa extracts using oligonucleotides complementary to the 5′ splice sites of exon 7 and exon 7B (oligonucleotides d and p, respectively; see Fig. 3). The duplex structure did not interfere detectably with oligonucleotide p-targeted cleavage of naked S678 RNA (data not shown). Moreover, in an extract pre-treated with an oligonucleotide against the 5′ end of U1 RNA, S678i and S678 RNAs were cleaved with similar efficiencies ($U1^-$; Fig. 8, lanes 1–3 and 7–9). These results suggest that base pairing between the 3′-terminal 5 nt of oligonucleotide p and free exon sequences probably leads to displacement of the RNA duplex to allow RNase H cleavage. Thus, the RNA structure apparently does not bias cleavage in favor of the distal 5′ splice site.

Following various periods of incubation in a mock-treated HeLa extract (0, 5, and 20 min at 30 °C), splicing mixtures were incubated with RNase H and oligonucleotides d and p (Fig. 8, lanes 4–6 and 10–12). At 20 min, the protection profiles obtained with S678i RNA

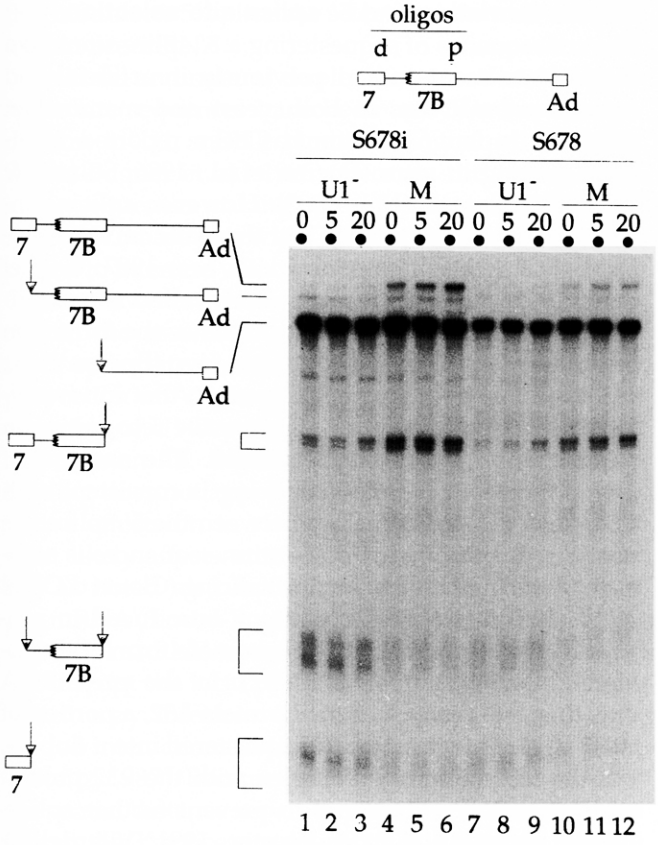

FIGURE 8. U1-dependent protection of competing 5′ splice sites. S678 and S678i RNAs were incubated at 30 °C for the indicated times (in min) in mock-treated (M) or U1 snRNP-depleted (U1⁻) HeLa nuclear extracts. Following incubation, oligonucleotides complementary to the 5′ splice sites of exons 7 (oligo d) and 7B (oligo p) were added along with RNase H. The position and diagram of fully protected pre-mRNAs or molecules derived from the cleavage at either the downstream, the upstream, or both 5′ splice sites are shown on the left.

indicated that 58% of protected pre-mRNA molecules arose from distal 5′ splice site protection only, whereas 42% arose from proximal protection (33% from protection at both sites and 9% from protection at the proximal site only) (Fig. 8, lane 6). Given that the 5′ splice site of exon 7 (AUG/GUAAGU) has a slightly better fit to the consensus than the 5′ splice site of exon 7B (GUG/GUAGGU), these values are consistent with the inferred strength of U1 snRNP binding to the two sequences. Following a 20-min incubation of S678 RNA, 72% of protected molecules were resistant to cleavage at the distal 5′ splice site only, compared to 28% arising from proximal protection (24% from protection at both sites and 4% from protection at the proximal site only) (Fig. 8, lane 12). For both transcripts, protection was eliminated almost completely when the assay was performed in the U1⁻ extract (Fig. 8, lanes 1–3 and 7–9). Our results therefore indicate that the assembly of U1-dependent complexes to the 5′ splice site of exon 7B is slightly less efficient when this 5′ splice site is sequestered into a duplex structure. Similar differences were observed when protection assays were performed in extracts depleted of ATP or U2 snRNP (data not shown), suggesting that duplex formation interferes directly with U1 snRNP binding. However, the fact that U1-dependent protection at the 5′ splice site of exon 7B was still detected despite much reduced splice site utilization suggests that the duplex structure may also affect other steps of spliceosome assembly.

DISCUSSION

Secondary structure in the alternative splicing unit of hnRNP A1

The mouse and human intron sequences separating alternative exon 7B from exon 8 in the pre-mRNA of hnRNP A1 contain several regions of similarity, suggesting that these conserved elements play a role in modulating the frequency of inclusion of exon 7B. A 200-nt region (STE) containing conserved elements CE6IO, CE7, and part of CE8 shifted splice site selection toward the distal 5′ splice site of exon 7 when located at its natural position downstream of the 5′ splice site of exon 7B. Using in vitro splicing assays to analyze the contribution of individual CE6IO, CE7, and CE8 elements, we found that the 84-nt CE6IO element displaced 5′ splice site selection to the same extent as the STE element. The role of STE and CE6IO in splice site selection was confirmed in vivo: deletion of STE from a mini-gene containing the complete hnRNP A1 alternative splicing unit mostly yielded transcripts containing exon 7B, whereas insertion of CE6IO restored skipping of exon 7B.

Several results suggest that CE6IO acts through the formation of a secondary structure rather than requiring the participation of a *trans*-acting factor. First, an excess of STE RNA did not affect the in vitro splicing of an STE-containing pre-mRNA. Second, an STE-containing A1 pre-mRNA migrated abnormally in

acrylamide/urea gels, and proper migration was restored by including 30% formamide in gels. Because this abnormal migration was not observed with STE RNA alone, our observations suggested that a portion of STE was involved in base pairing interactions with another portion of the pre-mRNA. Computer analysis predicted that CE6IO could make highly stable base pairing interactions with the 5′ splice site region of exon 7B. We have confirmed this model by showing that both CE6 and the sequences flanking the 5′ splice site of exon 7B are resistant to oligonucleotide-targeted RNase H cleavage. Likewise, removing the exon sequences proposed to base pair with CE6 activates splicing to exon 7B and renders CE6 sensitive to oligonucleotide-targeted RNase H cleavage. Finally, splicing to exon 7B was stimulated by introducing the complementary sequence of CE6 upstream of STE to sequester CE6 into an alternate duplex structure. Thus, our results are all in agreement and fully support a model in which the CE6IO region base pairs with the 5′ splice site region of exon 7B.

Because the CE6IO element was more efficient than the CE6 element alone at promoting distal 5′ splice site selection, the sequences flanking CE6 also contribute to the activity of CE6IO. The sequences immediately downstream of CE6 are relatively well-conserved and a portion of these may base pair with exon 7B to provide additional stability (Fig. 9). The sequences upstream of CE6, although diverging considerably between mouse and human, may nevertheless improve the stability of the duplex through the formation of additional base pairs both in the mouse and human pre-mRNAs (Fig. 9).

Duplex formation and 5′ splice site selection

The consequence of sequestering a 5′ splice site into a duplex has been studied previously in artificial and natural pre-mRNAs. In both yeast and mammalian systems, duplex formation has been reported to inhibit splicing in vitro (Eperon et al., 1986; Solnick & Lee, 1987; Goguel et al., 1993). However, splicing inhibition was considerably less dramatic in vivo (Eperon et al., 1986, 1988; Solnick & Lee, 1987; Goguel et al., 1993). These differences likely reflect the contribution of other processes that influence the formation or the stability of RNA duplexes in vivo (Eperon et al., 1988), and have led to the suggestion that in vivo effects of RNA duplexes on 5′ splice site recognition in natural pre-mRNAs may be slight. The analysis of β-tropomyosin pre-mRNA splicing is consistent with this view: duplex formation between the 5′ splice site of exon 6B and downstream intron sequences is associated with inhibition of in vitro splicing (Clouet d'Orval et al., 1991b), whereas mutations introduced to prevent duplex formation do not promote exon 6B inclusion in vivo (Libri et al., 1992). In the pre-mRNA encoding the yeast ribosomal protein L32, a portion of the 5′ splice site is naturally sequestered into a duplex, but the formation of a complex with the L32 protein and U1 snRNP is required to prevent further spliceosome assembly (Eng & Warner, 1991; Vilardell & Warner, 1994). In the case of the hnRNP A1 pre-mRNA, our results suggest that the duplex structure is formed in vivo. Experiments are in progress to address the possibility that factors modulate duplex formation in the A1 pre-mRNA. Thus, our study appears to represent the first example of a natural duplex structure

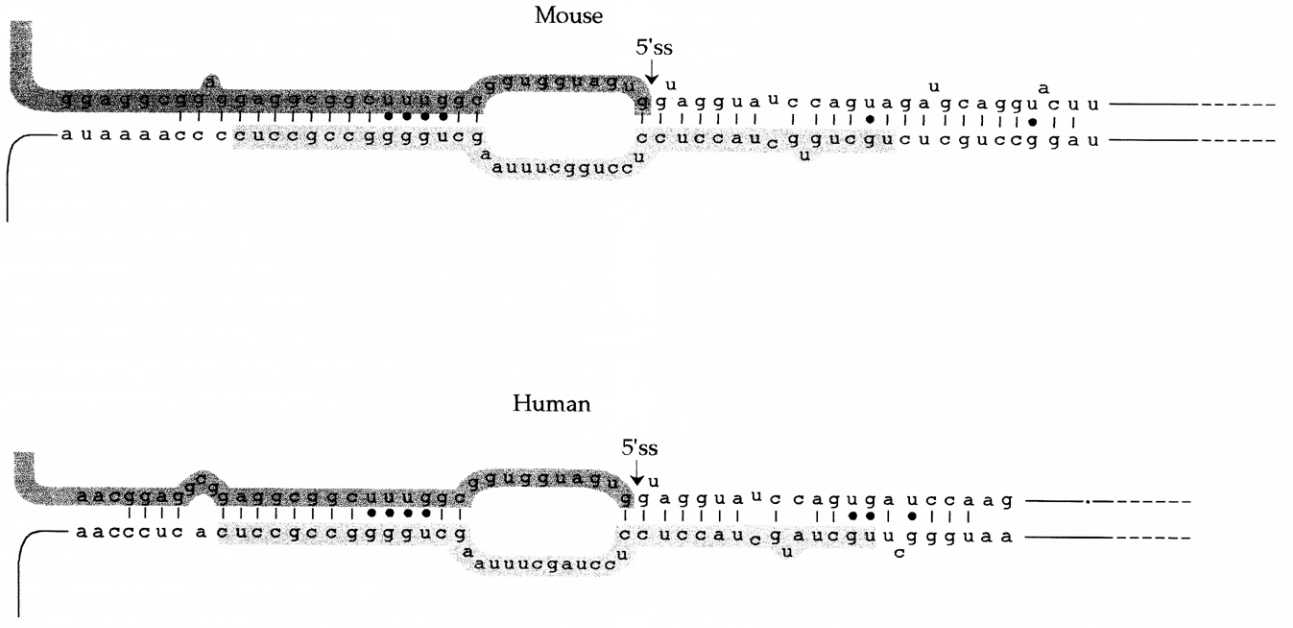

FIGURE 9. Comparison of base pairing interactions between CE6 and the 5′ splice site regions in mouse and human A1 pre-mRNAs. CE6 and exon sequences are represented by dark and light shaded boxes, respectively. The position of the 5′ splice site (5′ss) is indicated by the arrow.

that modulates 5′ splice site selection in vivo in a mammalian pre-mRNA.

Artificial and natural duplex structures involving 5′ splice site sequences have been associated with a reduction in U1 snRNP binding (Goguel et al., 1993; Sirand-Pugnet et al., 1995). Because the first 6 nt of intron sequences making up the 5′ splice site of hnRNP A1 exon 7B base pair with CE6, duplex formation is expected to interfere with their recognition by U1 snRNP. Consistent with this prediction, we observed a reduction in the assembly of U1-dependent complexes to the 5′ splice site of exon 7B. Nevertheless, a significant proportion of A1 pre-mRNA molecules sustained the assembly of U1-dependent complexes on the 5′ splice site of exon 7B. Because the decrease in U1 snRNP binding does not appear sufficient to explain the qualitative effects on in vitro splicing, duplex formation most likely affects other steps of spliceosome assembly, as noted also in the case of the β-tropomyosin pre-mRNA (Sirand-Pugnet et al., 1995). Successful binding of U1 snRNP to the 5′ splice site of exon 7B may not disrupt the local pre-mRNA structure completely, which may interfere with the establishment of extended interactions in the 5′ splice site region (Chabot & Steitz, 1987). Because duplex formation also reduces the spatial distance separating the 5′ splice site of exon 7 from the 3′ splice site of exon 8, it is possible that the closer proximity of the 5′ splice site of exon 7 also contributes to the observed shift in 5′ splice site selection in vitro and to exon 7B skipping in vivo.

Modulating exon 7B splicing

Recently, we have identified another conserved element (CE1) located in the middle of intron 7, upstream of the alternative exon 7B (Chabot et al., 1997). CE1 promotes upstream 5′ splice site selection when located at its natural position in between the 5′ splice sites of S1 RNA. CE1 also promotes exon 7B skipping in vivo, but less efficiently than CE6IO. Although the binding of hnRNP A1 to CE1 is required for the effect, CE1 does not affect U1 snRNP binding to competing 5′ splice sites. CE1 and CE6IO are not interchangeable because they require positioning downstream of exon 7 and 7B, respectively, to be fully active (Chabot et al., 1997 and data not shown). It is intriguing that at least two different mechanisms operate to modulate exon 7B skipping. The participation of two distinct elements may be important in vivo when considering that commitment likely occurs on nascent pre-mRNAs. CE1 may delay commitment between the 5′ splice site of exon 7 and the 3′ splice site of exon 7B. Following transcription of CE6IO and duplex formation, commitment between the 5′ splice site of exon 7 and the 3′ splice site of exon 8 would then be favored. Thus, the deletion of CE1 may stimulate 7/7B splicing, whereas the deletion of CE6IO may activate 7B/8 splicing. In both cases, removal of the remaining intron may occur by default, albeit inefficiently when the duplex structure is still present. Thus, the presence of both CE1 and CE6IO may be required to insure the efficient production of A1 mRNA lacking exon 7B.

The contribution of other intron conserved elements in altering splice site selection in the hnRNP A1 alternative splicing unit remains to be investigated. We may uncover elements that counteract or potentiate the effects of CE6IO and CE1, leading the way to a model that integrates a complex series of interactions modulating splice site selection in a simple alternative splicing unit.

MATERIALS AND METHODS

Plasmid constructions

pUC3-Fli-2 contains the hnRNP A1 genomic *Sal* I-*Eco*R I fragment from a BALB/c mouse (Ben-David et al., 1992). Intron 7B was sequenced using oligonucleotides A1893 (5′-TCCCTTCATCGGCCCAAAAT-3′), A1B1 (5′-TGGTGGACA GGGTTATGGAA-3′), and A1B4 (5′-CGGCTTCATTCTCTGA GTGA-3′). The GenBank accession number of the mouse hnRNP A1 alternative splicing unit is U65316.

The construction of pS1 is described in Chabot et al. (1997). The murine *Stu* I intron fragment was inserted into the *Eco*R V site of pKS Bluescript (Stratagene) to yield pSTE, or was inserted into the *Stu* I of pS1 to generate pS678. pSCE7 and pSCE8 (and i derivatives) were produced by direct insertion of reannealed oligonucleotides (22 bp and 27 bp for CE7 and CE8, respectively) into the *Stu* I site of pS1. Reannealed oligonucleotides corresponding to CE6 (41 bp) were inserted into the *Hinc* II site of pKS Bluescript to produce pCE6. A *Xho* I-*Hin*d III fragment from pCE6 was filled with Klenow and inserted into the *Stu* I site of pS1 to yield pSCE6 and pSCE6i. A *Sma* I-*Hae* III fragment from pSTE was inserted into the *Stu* I site of pS1 to produce pCE6Δ and pCE6Δi. To obtain pSCE6IO and pSCE6IOi, a *Stu* I-*Bbs* I fragment from pSTE was filled with Klenow and inserted into the *Stu* I site of pS1. The construction of pS6678 and pS6a678 was generated by subcloning the *Xho* I-*Hin*d III fragment of pCE6 into the *Sma* I site of pSTE after Klenow treatment to produce pK6678 and pK6a678. *Bam*H I-*Hin*d III fragments were then filled with Klenow and inserted into the *Stu* I site of pS1. The structure of the resulting plasmids was confirmed by extensive restriction enzyme analysis and DNA sequencing when appropriate.

The pmA1 vector was generated by inserting a genomic fragment of the mouse A1 gene (exon 5 to exon 10) (Ben-David et al., 1992) into pCMVSV (Yang et al., 1994). pmA1ΔSTE was obtained by deletion of the *Stu* I fragment in intron 7B. pmA1STEi and pmA1Δ1 were obtained by reinsertion of the *Stu* I fragment in the reverse orientation and by insertion of the *Stu* I-*Bbs* I fragment of STE, respectively.

Transcription and splicing assays

All plasmids were digested with *Sca* I to produce linear templates. Transcription was accomplished with T3 RNA polymerase (Pharmacia), in the presence of cap analogue and

[α-^{32}P] UTP (Amersham). RNA purification was performed as described (Chabot, 1994). ST and SF RNAs were produced by adding to transcription mixtures RNase H (Pharmacia) along with oligonucleotide A1B2 (ST-1, SF-1; 5′-CCTCCGC CTCCGTTGTTATA-3′) or oligonucleotide B (ST-2, SF-2; 5′-GCCAAAGCCGCCTC-3′).

Nuclear extracts were prepared as described (Dignam et al., 1992). Splicing mixtures were set up and processed as described in Krainer and Maniatis (1985). Splicing products were resolved in 6% (w/v) acrylamide/8 M urea/30% (v/v) formamide unless specified otherwise. The identity of lariat molecules was confirmed by performing debranching reactions in S100 extracts followed by migration in acrylamide/urea gels.

Expression vectors and transfection assays

Transfections in human HeLa and WI38VA13 cells was accomplished using the standard calcium-phosphate precipitation technique. After 48 h, RNA was extracted using the guanidium-HCl method (Chabot, 1994) and RT-PCR analysis was accomplished as described previously (Yang et al., 1994) using oligonucleotides CMV-1 and A1893 (Chabot et al., 1997).

RNase H assays

RNA incubated in splicing buffer (Krainer & Maniatis, 1985) were incubated at 37 °C for 30 min in the presence of 0.5 unit of RNase H (Pharmacia) and 5, 1, or 0.2 pmol/μL of either oligonucleotide A (5′-TTCCATAACCCTGTCCACCA-3′), B, C (5′-CTACTGGATACC-3′), CE6a (5′-GAGGCGGCCCCAG CTTAAAGCCAGGAGGAGGTAGCACAGCA-3′), CE7a (5′-AAGACAATCACTAACCACTCAT-3′), or CE8a (5′-TTGA AGGCCTTTATGTATTCCAGGTCA-3′).

When performed in the presence of nuclear extracts, RNase H and 25 pmol of oligonucleotides complementary to the 5′ splice sites of exons 7 and 7B (d: 5′-GAAACTTACCATC-3′ and p: 5′-GATACCTACCACTA-3′, respectively) were added to 10 μL splicing reactions after incubation for the specified times (Eperon et al., 1993). Incubation was continued for 15 min at 30 °C. HeLa extracts depleted in U1 snRNPs were produced by addition of RNase H and the oligonucleotide 5′-TCAGGTAAGTAT-3′ complementary to the 5′ end of U1 RNA. A mock-treated HeLa extract was obtained by incubation with RNase H and an unrelated oligonucleotide.

ACKNOWLEDGMENTS

We thank H. La Branche for sequencing the mouse intron 7B, J. Toutant for performing transfections, Y. Ben-David for providing the mouse genomic clone, and A. Lavigueur for comments on the manuscript. This work was supported by a grant from the Medical Research Council of Canada (MRCC). M.B. is the recipient of a MRCC Studentship. B.C. is a Chercheur-Boursier Junior II from the Fonds de la Recherche en Santé du Québec.

Received November 20, 1996; returned for revision December 19, 1996; revised manuscript received January 16, 1997

REFERENCES

Ben-David Y, Bani MR, Chabot B, De Koven A, Bernstein A. 1992. Retroviral insertions downstream of the heterogeneous nuclear ribonucleoprotein A1 gene in erythroleukemia cells: Evidence that A1 is not essential for cell growth. *Mol Cell Biol 12:4449–4455.*

Biamonti G, Buvoli M, Bassi MT, Morandi C, Cobianchi F, Riva S. 1989. Isolation of an active gene encoding human hnRNP protein A1. Evidence for alternative splicing. *J Mol Biol 207*:491–503.

Black DL. 1995. Finding splice sites within a wilderness of RNA. *RNA 1*:763–771.

Burd CG, Dreyfuss G. 1994. RNA binding specificity of hnRNP A1: Significance of hnRNP A1 high-affinity binding sites in pre-mRNA splicing. *EMBO J 13*:1197–1204.

Buvoli M, Cobianchi F, Bestagno MG, Mangiarotti A, Bassi MT, Biamonti G, Riva S. 1990. Alternative splicing in the human gene for the core protein A1 generates another hnRNP protein. *EMBO J 9*:1229–1235.

Cáceres JF, Stamm S, Helfman DM, Krainer AR. 1994. Regulation of alternative splicing in vivo by overexpression of antagonistic splicing factors. *Science 265*:1706–1709.

Chabot B. 1994. Synthesis and purification of RNA substrates. In: Higgins SJ, Hames BD, eds. *RNA processing, vol I.* Oxford, Oxford University Press.

Chabot B. 1996. Directing alternative splicing: Cast and scenarios. *Trends Genet 12*:472–478.

Chabot B, Blanchette M, Lapierre I, La Branche H. 1997. An intron element modulating 5′ splice site selection in the hnRNP A1 pre-mRNA interacts with hnRNP A1. *Mol Cell Biol*. Forthcoming.

Chabot B, Steitz JA. 1987. Multiple interactions between the splicing substrate and small nuclear ribonucleoproteins in spliceosomes. *Mol Cell Biol 7*:281–293.

Charpentier B, Rosbash M. 1996. Intramolecular structure in yeast introns aids the early steps of in vitro spliceosome assembly. *RNA 2*:509–522.

Chebli K, Gattoni R, Schmitt P, Hildwein G, Stevenin J. 1989. The 216-nucleotide intron of the E1A pre-mRNA contains a hairpin structure that permits utilization of unusually distant branch acceptors. *Mol Cell Biol 9*:4852–4861.

Clouet d'Orval B, d'Aubenton-Carafa Y, Marie J, Brody E. 1991a. Determination of an RNA structure involved in splicing inhibition of a muscle-specific exon. *J Mol Biol 221*:837–856.

Clouet d'Orval B, d'Aubenton-Carafa Y, Sirand-Pugnet P, Brody E, Marie J. 1991b. RNA secondary structure represses utilization of a muscle-specific exon in HeLa cell nuclear extracts. *Science 252*:1823–1828.

Deshler JO, Rossi JJ. 1991. Unexpected point mutations activate cryptic 3′ splice sites by perturbing a natural secondary structure within a yeast intron. *Genes & Dev 5*:1252–1263.

Dignam JD, Lebovitz RM, Roeder RG. 1992. Accurate transcription initiation by RNA polymerase II in a soluble extract from isolated mammalian nuclei. *Nucleic Acids Res 11*:1475–1489.

Domenjoud L, Gallinaro H, Kister L, Meyer S, Jacob M. 1991. Identification of a specific exon sequence that is a major determinant in the selection between a natural and a cryptic 5′ splice site. *Mol Cell Biol 11*:4581–4590.

Eng FJ, Warner JR. 1991. Structural basis for the regulation of splicing of a yeast messenger RNA. *Cell 65*:797–804.

Eperon IC, Ireland DC, Smith RA, Mayeda A, Krainer AR. 1993. Pathways for selection of 5′ splice sites by U1 snRNPs and SF2/ASF. *EMBO J 12*:3607–3617.

Eperon LP, Estibeiro JP, Eperon IC. 1986. The role of nucleotide sequences in splice site selection in eukaryotic pre-messenger RNA. *Nature 324*:280–282.

Eperon LP, Graham IR, Griffiths AD, Eperon IC. 1988. Effects of RNA secondary structure on alternative splicing of pre-mRNA: Is folding limited to a region behind the transcribing RNA polymerase? *Cell 54*:393–401.

Fu XD. 1995. The superfamily of arginine/serine-rich splicing factors. *RNA 1*:663–680.

Fu XY, Colgan JD, Manley JL. 1988. Multiple cis-acting sequence elements are required for efficient splicing of simian virus 40 small-t antigen pre-mRNA. *Mol Cell Biol 8*:3582–3590.

Goguel V, Rosbash M. 1993. Splice site choice and splicing efficiency are positively influenced by pre-mRNA intramolecular base pairing in yeast. *Cell 72*:893–901.

Goguel V, Wang Y, Rosbach M. 1993. Short artificial hairpins sequester splicing signals and inhibit yeast pre-mRNA splicing. *Mol Cell Biol 13*:6841–6848.

Kister L, Domenjoud L, Gallinaro H, Jacob M. 1993. A cis-acting selector of a 5′ splice site. *J Biol Chem 268*:21955–21961.

Kohtz JD, Jamison SF, Will CL, Zuo P, Lührmann R, Garcia-Blanco MA, Manley JL. 1994. Protein–protein interactions and 5′-splice-site recognition in mammalian mRNA precursors. *Nature 368*:119–124.

Krainer AR, Maniatis T. 1985. Multiple factors including the small nuclear ribonucleoproteins U1 and U2 are necessary for pre-mRNA splicing in vitro. *Cell 42*:725–736.

Lavigueur A, La Branche H, Kornblihtt AR, Chabot B. 1993. A splicing enhancer in the human fibronectin alternate ED1 exon interacts with SR proteins and stimulates U2 snRNP binding. *Genes & Dev 7*:2405–2417.

Libri D, Balvay L, Fizman MY. 1992. In vivo splicing of the β tropomyosin pre-mRNA: A role for branch point and donor site competition. *Mol Cell Biol 12*:3204–3215.

Libri D, Stutz F, McCarthy T, Rosbach M. 1995. RNA structural patterns and splicing: Molecular basis for an RNA-based enhancer. *RNA 1*:425–436.

Lin CH, Patton JG. 1995. Regulation of alternative 3′ splice site selection by constitutive splicing factors. *RNA 1*:234–245.

Liu HX, Goodall GJ, Kole R, Filipowicz W. 1995. Effects of secondary structure on pre-mRNA splicing: Hairpins sequestering the 5′ but not the 3′ splice site inhibit intron processing in *Nicotiana plumbaginifolia*. *EMBO J 14*:377–388.

Manley JL, Tacke R. 1996. SR proteins and splicing control. *Genes & Dev 10*:1569–1579.

Mayeda A, Krainer AR. 1992. Regulation of alternative pre-mRNA splicing by hnRNP A1 and splicing factor SF2. *Cell 68*:365–375.

Mayeda A, Munroe SM, Cáceres JF, Krainer AR. 1994. Function of conserved domains of hnRNP A1 and other hnRNP A/B proteins. *EMBO J 13*:5483–5495.

Newman A. 1987. Specific accessory sequences in *Saccharomyces cerevisiae* introns control assembly of pre-mRNAs into spliceosomes. *EMBO J 6*:3833–3839.

Reed R. 1996. Initial splice-site recognition and pairing during pre-mRNA splicing. *Curr Opin Genet Dev 6*:215–220.

Robberson BL, Cote GJ, Berget SM. 1990. Exon definition may facilitate splice site selection in RNAs with multiple exons. *Mol Cell Biol 10*:84–94.

Siebel CW, Admon A, Rio DC. 1995. Soma-specific expression and cloning of PSI, a negative regulator of P element pre-mRNA splicing. *Genes & Dev 9*:269–283.

Siebel CW, Kanaar R, Rio DC. 1994. Regulation of tissue-specific P-element pre-mRNA splicing requires the RNA-binding protein PSI. *Genes & Dev 8*:1713–1725.

Sirand-Pugnet P, Durosay P, Clouet d'Orval B, Brody E, Marie J. 1995. β-Tropomysosin pre-mRNA folding around a muscle-specific exon interferes with several steps of spliceosome assembly. *J Mol Biol 251*:591–602.

Solnick D. 1985. Alternative splicing caused by RNA secondary structure. *Cell 43*:667–676.

Solnick D, Lee SI. 1987. Amount of RNA secondary structure required to induce an alternative splice. *Mol Cell Biol 7*:3194–3198.

Valcárcel J, Singh R, Zamore PD, Green MR. 1993. The protein Sex-lethal antagonizes the splicing factor U2AF to regulate alternative splicing of transformer pre-mRNA. *Nature 362*:171–175.

Vilardell J, Warner JR. 1994. Regulation of splicing at an intermediate step in the formation of the spliceosome. *Genes & Dev 8*:211–220.

Wang Z, Hoffmann HM, Grabowski PJ. 1995. Intrinsic U2AF binding is modulated by exon enhancer signals in parallel with changes in splicing activity. *RNA 1*:21–35.

Wu JY, Maniatis T. 1993. Specific interactions between proteins implicated in splice site selection and regulated alternative splicing. *Cell 75*:1061–1070.

Yang X, Bani MR, Lu SJ, Rowan S, Ben-David Y, Chabot B. 1994. The A1 and $A1^B$ proteins of heterogeneous nuclear ribonucleoparticles modulate 5′ splice site selection in vivo. *Proc Natl Acad Sci USA 91*:6924–6928.

Zuo P, Maniatis T. 1996. The splicing factor $U2AF^{35}$ mediates critical protein–protein interactions in constitutive and enhancer-dependent splicing. *Genes & Dev 10*:1356–1368.